Reaction kinetics of Cl atoms with limonene: An experimental and theoretical study

ARTICLE *in* ATMOSPHERIC ENVIRONMENT · DECEMBER 2014

Impact Factor: 3.28 · DOI: 10.1016/j.atmosenv.2014.09.066

2 AUTHORS:

Manas Dash
National Chiao Tung University
10 PUBLICATIONS **44** CITATIONS
SEE PROFILE

B. Rajakumar
Indian Institute of Technology Madras
37 PUBLICATIONS **244** CITATIONS
SEE PROFILE

Atmospheric Environment 99 (2014) 183–195

Contents lists available at ScienceDirect

Atmospheric Environment

journal homepage: www.elsevier.com/locate/atmosenv

Reaction kinetics of Cl atoms with limonene: An experimental and theoretical study

Manas Ranjan Dash, B. Rajakumar*

Department of Chemistry, Indian Institute of Technology Madras, Chennai 600036, India

HIGHLIGHTS

- First kinetic study of the reaction of Cl atoms with limonene as a function of temperature.
- Additions and abstraction kinetics of limonene by Cl atom were discussed.
- Atmospheric lifetime of limonene was computed.

GRAPHICAL ABSTRACT

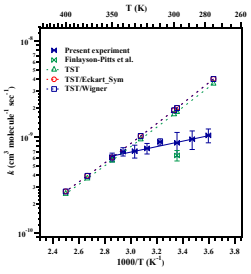

ARTICLE INFO

Article history:
Received 29 March 2014
Received in revised form
8 September 2014
Accepted 25 September 2014
Available online 26 September 2014

Keywords:
Limonene
Cl atoms
Rate coefficient
Relative rate technique
Conventional transition-state theory (CTST)
Atmospheric lifetime

ABSTRACT

Rate coefficients for the reaction of Cl atoms with limonene ($C_{10}H_{16}$) were measured between 278–350 K and 800 Torr of N_2, using the relative rate technique, with 1,3-butadiene (C_4H_6), n-nonane (C_9H_{20}), and 1-pentene (C_5H_{10}) as reference compounds. Cl atoms were generated by UV photolysis of oxalyl chloride ($(COCl)_2$) at 254 nm. A gas chromatograph equipped with a flame ionization detector (GC-FID) was used for quantitative analysis of the organics. The rate coefficient for the reaction of Cl atoms with limonene at 298 K was measured to be $(8.65 \pm 2.44) \times 10^{-10}$ cm^3 molecule^{-1} s^{-1}. The rate coefficient is an average value of the measurements, with two standard deviations as the quoted error, including uncertainties in the reference rate coefficients. The kinetic data obtained over the temperature range of 278–350 K were used to derive the following Arrhenius expression: $k(T) = (9.75 \pm 4.1) \times 10^{-11}$ exp[$(655 \pm 133)/T$] cm^3 molecule^{-1} s^{-1}. Theoretical kinetic calculations were also performed for the title reaction using conventional transition state theory (CTST) in combination with G3(MP2) theory between 275 and 400 K. The kinetic data obtained over the temperature range of 275–400 K were used to derive an Arrhenius expression: $k(T) = (7.92 \pm 0.82) \times 10^{-13}$ exp[$(2310 \pm 34)/T$] cm^3 molecule^{-1} s^{-1}. The addition channels contributes maximum to the total reaction and H-abstraction channels can be neglected in the range of studied pressures. The Atmospheric lifetime (τ) of limonene due to its reaction with Cl atoms was estimated and concluded that the reaction with chlorine atoms can be an effective tropospheric loss pathway in the marine boundary layer and in coastal urban areas.

1. Introduction

Biogenic volatile organic compounds (BVOCs), those are released into the troposphere react mainly with hydroxyl radical (OH) which is major tropospheric oxidant. Chlorine atoms (Cl) are also known to contribute significantly in the oxidative capacity of the troposphere particularly in the early morning (Thornton et al.,

* Corresponding author.
E-mail addresses: rajakumar@iitm.ac.in, ballarajakumar@gmail.com (B. Rajakumar).

http://dx.doi.org/10.1016/j.atmosenv.2014.09.066
1352-2310/

2010). Cl atoms react rapidly with BVOCs approximately about 10–100 times faster than corresponding OH radical reactions. Cl atoms can react with BVOCs by two competitive processes. First one is Cl atom addition to the carbon–carbon double bond to form chloroalkyl radicals and the second one is abstraction of a hydrogen atom to form an alkyl radical and HCl. Abstraction reaction is an endothermic process with estimated activation energy of (3–7) kcal mol^{-1} (Stevens and Spicer, 1977; Lee and Rowland, 1977; Parmar and Benson, 1988; Dobis and Benson, 1991; Kaiser and Wallington, 1996; Pilgrim and Taatjes, 1997), whereas, addition reaction is an exothermic process and proceeds through a little or

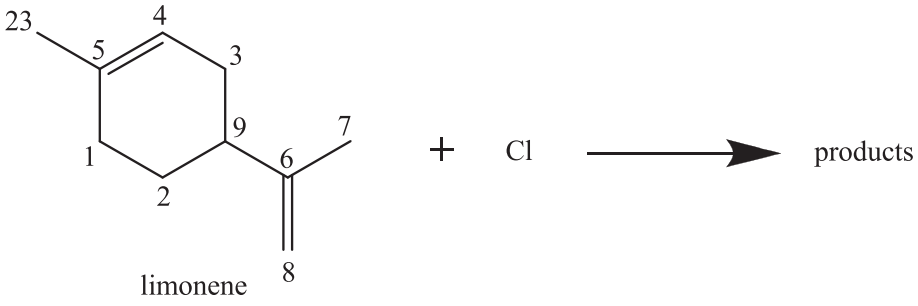

no activation barrier (Stevens and Spicer, 1977). Therefore, at lower temperatures (<500 K), addition reaction is dominated over abstraction reaction, and at higher temperatures the abstraction reaction is more important than addition reaction. Although the global average concentration of Cl atoms is only about 10^3 atoms cm^{-3} (Singh et al., 1996; Wingenter et al., 1999), which is three orders of magnitude lower than the global average OH concentration i.e., 10^6 radicals cm^{-3} (Prinn et al., 1995), it is significantly higher in the marine boundary layer (MBL), coastal regions, reaching a peak concentration of about 10^5 atoms cm^{-3} (Spicer et al., 1998). The main source of chlorine atoms is the photolysis of chlorine containing compounds generated in the sea-salt aerosols (Spicer et al., 1998; George et al., 2010). Recently, nitryl chloride ($ClNO_2$) was observed to be a gaseous photolytic Cl atom precursor (Ravishankara, 2009; Thornton et al., 2010; Glasow, 2010), which is formed in the night-time reaction of N_2O_5 with chloride-containing aerosol (Osthoff et al., 2008). The interaction of biogenic compounds with chlorine atoms can occur when sea breezes carry marine air masses inland and some biogenic compounds such as isoprene are expected to be emitted by the oceans as well (Bonsang et al., 1992; Moore et al., 1994; Milne et al., 1995; McKay et al., 1996; Ratte et al., 1998). These organics also can react with OH radicals during the day time, NO_3 at night time, and O_3 during both day and night times.

Limonene [4-isopropenyl-1-methyl-cyclohexene] is a naturally occurring monocyclic monoterpene emitted from vegetation. The purpose of this work is to study the kinetics of chlorine atoms with limonene as a function of temperature and pressure. This work provides the first kinetic data for the reaction of limonene with chlorine atoms as a function of temperature. To the best of our knowledge, only one investigation on Cl atom reaction with limonene is available in the literature (Finlayson-Pitts et al., 1999) at room temperature. Finlayson-Pitts et al. (1999) carried out the reaction at 298 K and 1 atm pressure using relative rate technique. The reported rate coefficient (in the units of cm^3 $molecule^{-1}$ s^{-1}) is: k (limonene + Cl) = (6.4 ± 0.8) × 10^{-10}. Temperature dependent rate coefficients for this reaction are not available in the literature till to date, to the best of our knowledge. In addition, theoretical calculations of the potential energy surfaces for this reaction at various levels of theory are also presented to provide some additional insights into the energetics. The rate coefficients are also computed using conventional transition-state theory (CTST) in combination with Wigner's and Eckart's symmetrical tunneling methods in the temperature range of 275–400 K. The computed temperature dependent rate coefficients are compared with the experimentally measured rate coefficients and the available literature value at room temperature. The data obtained in this work were used to estimate the effective lifetime of limonene in the troposphere.

2. Experimental and computational methods

2.1. Room temperature study

Reactions were carried out in a quartz reaction chamber of ~1750 cm^3 volume at 298 K and ~800 Torr of N_2/Air. The details of the experimental set-up are given elsewhere (Dash and Rajakumar, 2013; Dash et al., 2013) and only a brief description is given here. Cl atoms were generated by photolysis of oxalyl chloride ($(COCl)_2$) at 254 nm, using two UV lamps (SANKYO DENKI G8T5, 8 W).

$$(COCl)_2 + h\upsilon\ (\approx 254\ nm) \rightarrow 2Cl + 2CO$$

The reaction mixtures, consisting of limonene, 1,3-butadiene as a reference compound, oxalyl chloride, and nitrogen were prepared in the reaction chamber, using a vacuum manifold system. The prepared reaction mixtures were kept for 30–45 min for equilibration before photolysis, which was confirmed by repeatability of the gas chromatogram. The mixtures were photolyzed for a period of 30 s, in steps of 10 s, and after each photolysis step the decrease in the concentration of the limonene and the 1,3-butadiene were determined, using gas chromatograph (Agilent Technologies 6890N), with a flame ionization detector (FID). A sample of 300 μL was transferred from the reaction chamber (~2 L volume) to GC, using a gas-tight syringe in each GC analysis and which is negligible compared to the total volume of the reaction chamber. Therefore, the change in volume and concentration due to sampling in order to analyze the reaction mixture with GC/FID is negligible. The GC column used in this experiment was a capillary column (HP-5, 30 m × 0.320 mm × 0.25 μm, 19091J-413) run at 75 °C constant oven temperature. The column was operated at GC inlet temperature of 160 °C and detector temperature of 170 °C.

2.2. Temperature dependence study

The experiments were carried out in a double-walled Pyrex reaction chamber of ~1250 cm^3 volume closed at both ends by UV fused silica broadband precision windows (50.8 mm diameter, THORSLABS). The temperature in the reaction cell was maintained

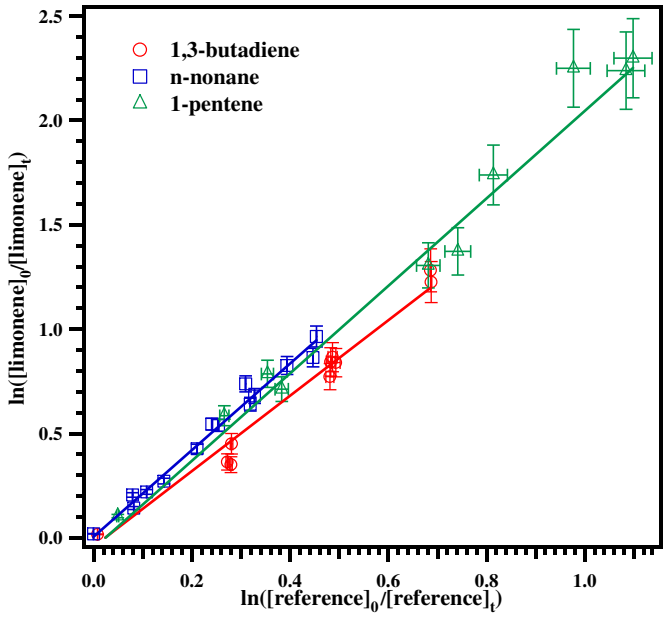

Fig. 1. Plot of the relative decrease in the concentration of limonene due to its reaction with Cl atom at 298 K in N_2.

by circulating heated/cooled fluid in the jacketed portion of the cell. A type K thermocouple was used to read the temperature inside the reaction chamber. The gas temperature inside the chamber did not differ from the temperature of the circulating fluid by more than 2 K in the studied temperature range. The title reaction was investigated over the pressure range of 700–850 Torr of $N_2/N_2–O_2$ and the temperature range of 278–350 K. n-nonane and 1-pentene were chosen as reference compounds for the title reaction for the investigation of temperature dependence of the reaction. The initial concentration ranges used in the experiments were 3×10^{16}–1.2×10^{17} molecules cm^{-3} for the reactants, 1.7×10^{15}–4.7×10^{16} molecules cm^{-3} for reference compounds, and 7.8×10^{16}–5.2×10^{17} molecules cm^{-3} for $(COCl)_2$.

The kinetic data were obtained from the measurement of the simultaneous loss of reactant and reference compound, using the standard expression.

$$\ln\left(\frac{[\text{reactant}]_0}{[\text{reactant}]_t}\right) = \left(\frac{k_{\text{reactant}}}{k_{\text{reference}}}\right)\ln\left(\frac{[\text{reference}]_0}{[\text{reference}]_t}\right) \quad (1)$$

where $[\text{reactant}]_0$ and $[\text{reference}]_0$ are the initial concentrations of reactant and reference compounds and $[\text{reactant}]_t$ and $[\text{reference}]_t$ are corresponding concentrations at time t.

The relative rate method relies on the assumption that both the reactant and the reference compounds are removed solely by reaction with Cl atoms. To verify this assumption, mixtures of reactant and reference compounds $(COCl)_2$ and nitrogen were prepared in the reaction cell and allowed to mix in the dark for about 5 h, and the concentration of the components were monitored by GC at different time intervals. There was no significant decrease in the concentration of any of the molecules, indicating the absence of dark reactions as well as wall losses. To test for possible photolysis of the reactants, a mixture of reactant and reference compounds, and nitrogen were photolyzed for 30 min in the absence of $(COCl)_2$. There was no significant decrease in the concentration of the reactant and reference compounds, and also no other products were observed which confirmed the absence of any loss due to direct photolysis.

2.3. Chemicals

(S)-(−)-Limonene (purity 96%, Sigma Aldrich), 1,3-butadiene (purity 99.5%, PRAXAIR), n-nonane (purity 99%, Sigma Aldrich), 1-pentene (purity 98.5%, Sigma Aldrich), oxalyl chloride (purity 98%, SPECTROCHEM), nitrogen (99.995%), zero air (98%), and oxygen (98%). (S)-(−)-Limonene, oxalyl chloride, n-nonane, 1-pentene, and were subjected to repeated freeze–pump–thaw cycles, before use.

2.4. Computational methodology

The Gaussian 09 program (Frisch et al., 2010) suit was used to carry out all the calculations in these studies. The geometries of the reactants, intermediates (I_{adds}), transition states (TSs), and products of all possible addition and abstraction channels were optimized with the second-order Møller-Plesset (1934) MP2(FULL) level of theory including all electrons in correlation with the Pople basis set 6-31G(d). The rate coefficients for the title reaction were computed using conventional transition-state theory (CTST) (Wright, 1999).

$$k(T) = l\frac{k_B T}{h}\left(\frac{Q_{\ddagger}}{Q_R}\right)\exp\left(-\frac{\Delta E^{\ddagger}}{RT}\right) \quad (2)$$

where, l is the reaction path degeneracy, ‡ represents the transition state, h is Planck's constant, and k_B is the Boltzmann constant. $Q_{\ddagger}$ and Q_R are partition functions for the transition state and the

Table 1
Relative rate measurements of Cl atom reaction with limonene at 298 K in N_2/Air, using 1,3-butadiene as a reference compound.

Buffer gas	P (Torr)	$(k_{\text{limonene}}/k_{\text{1,3-butadiene}})$[a]	$k \times 10^{10}$ [b] (cm^3 $molecule^{-1}$ s^{-1})	Literature (298 K) $k \times 10^{10}$ (cm^3 $molecule^{-1}$ s^{-1})
N_2	805	1.58 ± 0.17	6.64 ± 0.95	6.4 ± 0.8
N_2	806	1.80 ± 0.09	7.56 ± 0.81	(Finlayson-Pitts et al., 1999).
N_2	806	1.79 ± 0.12	7.52 ± 0.88	
N_2	801	1.79 ± 0.15	7.52 ± 0.95	
		1.74 ± 0.28	**7.31 ± 1.81**	
N_2	705	2.09 ± 0.32	8.78 ± 1.58	
N_2	599	1.80 ± 0.12	7.56 ± 0.88	
N_2	403	1.72 ± 0.13	7.22 ± 0.88	
N_2	205	2.01 ± 0.11	8.44 ± 0.93	
Air	800	2.27 ± 0.30	9.53 ± 1.55	
Air	802	2.18 ± 0.10	9.16 ± 0.97	
Air	804	2.38 ± 0.07	10.0 ± 1.0	
Air	798	2.08 ± 0.26	8.74 ± 1.37	
Air	812	1.97 ± 0.12	8.27 ± 0.94	
		2.18 ± 0.43	**9.16 ± 2.67**	

[a] Indicated errors are two least-squares standard deviations.
[b] Indicated errors are two least-squares standard deviations and include uncertainties in the rate coefficients of $k_{\text{1,3-butadiene}}$ (Ragains and Finlayson-Pitts, 1997).

reactants. $\Delta E_0^{\ddagger}$ is the classical barrier height, and R is Universal gas constant. The two spin-orbit (SO) states $^2p_{3/2}$ (lowest) and $^2p_{1/2}$ of Cl having degeneracies of 4 and 2, respectively, and separated by 882.3515 cm^{-1} (Chase, 1998) were included in the electronic partition function calculations. Quantum mechanical tunneling effects along the reaction coordinates are included by temperature dependent transmission coefficient $\Gamma(T)$. The final rate coefficients were calculated using the equation

$$k_{\Gamma}(T) = \Gamma(T) \times k(T) \quad (3)$$

The values of $\Gamma(T)$ were calculated by using two methods namely Wigner's method (Wigner, 1937; Dash and Rajakumar, 2012) and Eckart's Symmetrical method (Eckart, 1930; Johnston and Heicklen, 1962; Dash and Rajakumar, 2012).

3. Results and discussion

3.1. Experimental

Fig. 1 depicts a typical experimental plot derived from the analysis of relative rate measurements. The rate coefficients for the reaction of limonene with Cl atom and two different bath gases at room temperature, studied in this work, are summarized in Table 1. For each experiment, slope and errors were obtained from the linear least-square fitting of the data. The weighted average value of the rate coefficients for individual measurements is shown in **bold** letters in Table 1. The quoted errors are two least-squares standard deviations and include uncertainties associated with the rate coefficients of reference compound. As shown in Table 1, the mean value of the slopes is $k_{limonene}/k_{1,3\text{-butadiene}} = 1.74 \pm 0.28$ in N_2. From this slope, using $k_{1,3\text{-butadiene}} = (4.2 \pm 0.4) \times 10^{-10}$ cm^3 $molecule^{-1}$ s^{-1} (Ragains and Finlayson-Pitts, 1997) at 298 K, the rate coefficient for the reaction of limonene with Cl atoms was determined to be $k_{limonene} = (7.31 \pm 1.81) \times 10^{-10}$ cm^3 $molecule^{-1}$ s^{-1} at 298 K. The measurements at pressures, 705, 599, 403 and 205 Torr, indicate that the slopes are independent of the total pressure in this range. To the best of our knowledge, only one experimentally measured rate coefficient is available in the literature for the reaction of limonene with Cl atom. Finlayson-Pitts et al. (1999) measured the rate coefficient for the reaction of Cl atom with limonene and reported it to be $k_{limonene} = (6.4 \pm 0.8) \times 10^{-10}$ cm^3 $molecule^{-1}$ s^{-1} using relative rate technique, which is in good agreement with the present experimentally measured rate coefficient at room temperature. Experiments were also carried out in the presence of air and the mean value of the slops is $k_{limonene}/k_{1,3\text{-butadiene}} = 2.18 \pm 0.43$. The rate coefficient determined from this value is $k_{limonene} = (9.16 \pm 2.67) \times 10^{-10}$ cm^3 $molecule^{-1}$ s^{-1}, which shows a marginal increase in the rate coefficient is possible in the presence of air (Table 1), *vide infra*.

The temperature dependence of the reaction of Cl atoms with limonene was investigated over the temperature range of 278–350 K, using n-nonane and 1-pentene as reference compounds. It has been reported that the rate coefficients of the reactions of Cl atoms with simple alkanes has insignificant

Table 2
Rate coefficient ratios and rate coefficients (units: cm^3 $molecule^{-1}$ s^{-1}) of Cl atoms with limonene over the temperature range of 278–350 K and at 700–800 Torr in N_2.

T (K)	Reference	$(k_{limonene}/k_{ref})$[a]	$(k_{limonene}/k_{ref})_{avr}$	$k \times 10^{10}$ [b]	$k_{avr} \times 10^{10}$	Literature (298 K) $k \times 10^{10}$
278	n-nonane	2.27 ± 0.22 2.33 ± 0.46	2.30 ± 0.51	9.89 ± 2.19	10.35 ± 1.70	6.4 ± 0.8 (Finlayson-Pitts et al., 1999).
	1-pentene	1.84 ± 0.31 2.03 ± 0.32 1.91 ± 0.11	1.93 ± 0.46	10.8 ± 1.08		
288	n-nonane	2.26 ± 0.23 2.13 ± 0.41	2.20 ± 0.48	9.44 ± 2.07	9.44 ± 2.07	
298	n-nonane	2.03 ± 0.11 2.07 ± 0.06 1.73 ± 0.16[c]	2.05 ± 0.13	8.82 ± 0.58	8.65 ± 2.44	
	1-pentene	1.92 ± 0.13 2.09 ± 0.12 2.21 ± 0.10 2.15 ± 0.32	2.09 ± 0.37	9.81 ± 1.17		
	1,3-butadiene	1.58 ± 0.17 1.80 ± 0.09 1.79 ± 0.12 1.79 ± 0.15	1.74 ± 0.28	7.31 ± 1.81		
310	n-nonane	2.09 ± 0.12 2.03 ± 0.09	2.06 ± 0.15	8.86 ± 0.67	8.86 ± 0.67	
320	n-nonane	1.72 ± 0.21 1.67 ± 0.12	1.70 ± 0.24	7.29 ± 1.05	7.57 ± 0.95	
	1-pentene	1.88 ± 0.16 1.95 ± 0.10 2.12 ± 0.13	1.98 ± 0.23	7.85 ± 0.98		
330	n-nonane	1.59 ± 0.21 1.71 ± 0.13	1.65 ± 0.25	7.10 ± 1.09	7.10 ± 1.09	
340	n-nonane	1.47 ± 0.09 1.65 ± 0.09	1.56 ± 0.13	6.71 ± 0.57	7.01 ± 0.70	
	1-pentene	2.17 ± 0.16 2.10 ± 0.12 2.06 ± 0.07	2.11 ± 0.19	7.30 ± 0.39		
350	n-nonane	1.35 ± 0.07 1.50 ± 0.10 1.68 ± 0.07[c]	1.43 ± 0.14	6.13 ± 0.63	6.13 ± 0.63	

[a] Indicated errors are two least-squares standard deviations.
[b] Indicated errors are two least-squares standard deviations and include uncertainties in the rate coefficients of $k_{1,3\text{-butadiene}}$ (Ragains and Finlayson-Pitts, 1997) and $k_{n\text{-nonane}}$ (Aschmann and Atkinson, 1995) and do not include uncertainties in the rate coefficients of $k_{1\text{-pentene}}$ (Coquet and Ariya, 2000).
[c] Experiments carried out in presence of O_2.

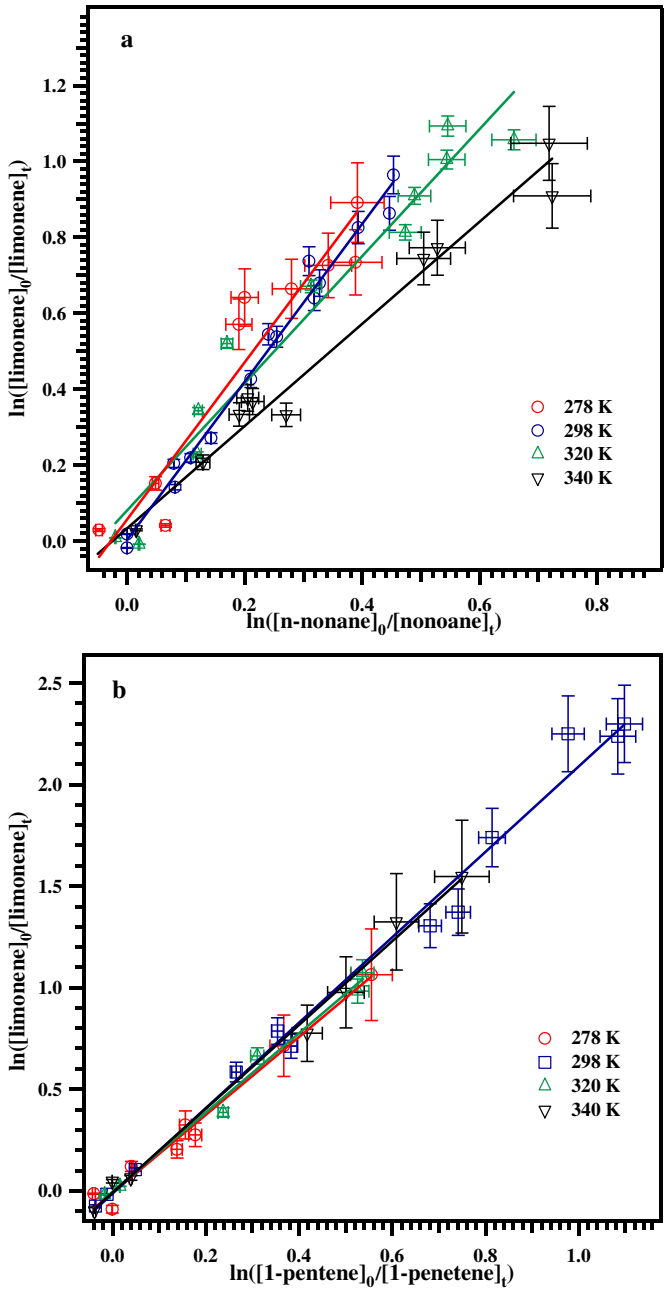

Fig. 2. Plots of the relative decrease in the concentration of limonene due to its reaction with Cl atoms at 278, 298, 320, and 340 K in N_2 with (a) n-nonane and (b) 1-pentene as reference compounds.

temperature dependence (Lewis et al., 1980). So, we have used the room temperature rate coefficient of n-nonane + Cl reaction reported by Aschmann and Atkinson (1995) ($k_{\text{n-nonane}} = (4.3 \pm 0.1) \times 10^{-10}$ cm^3 molecule^{-1} s^{-1}) for the reference reaction over the temperature range of 278–350 K. Coquet and Ariya (2000) studied the rate coefficients of Cl atoms with 1-pentene over the temperature range of 283–323 K in air and N_2 at atmospheric pressure of 760 Torr. We have used the rate coefficient for the reaction of Cl with 1-pentene reported by Coquet and Ariya (2000) $k_{\text{1-pentene}} = (4.0 \pm 2.2) \times 10^{-11}$ exp{−(−6.1 ± 2.4) × 1000/RT} cm^3 molecule^{-1} s^{-1} in the present experiments. This work provides the first kinetic study for the reaction of Cl atom with limonene as a function of temperature. The relative rate coefficients were measured at 278, 288, 298, 310, 320, 330, 340,

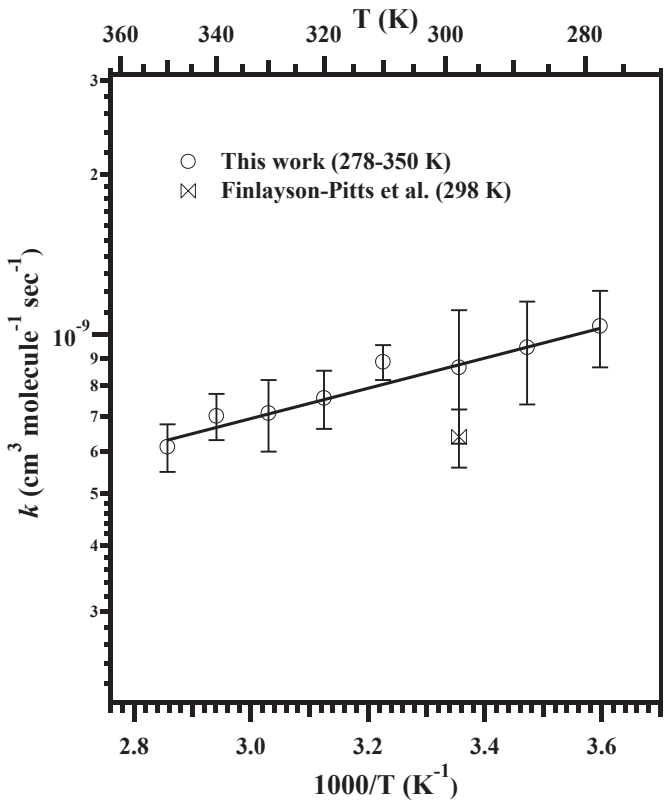

Fig. 3. Arrhenius plot for the rate coefficient data obtained for the Cl atom reaction with limonene over the temperature range of 278–350 K. The indicated errors are the two least-squares standard deviations.

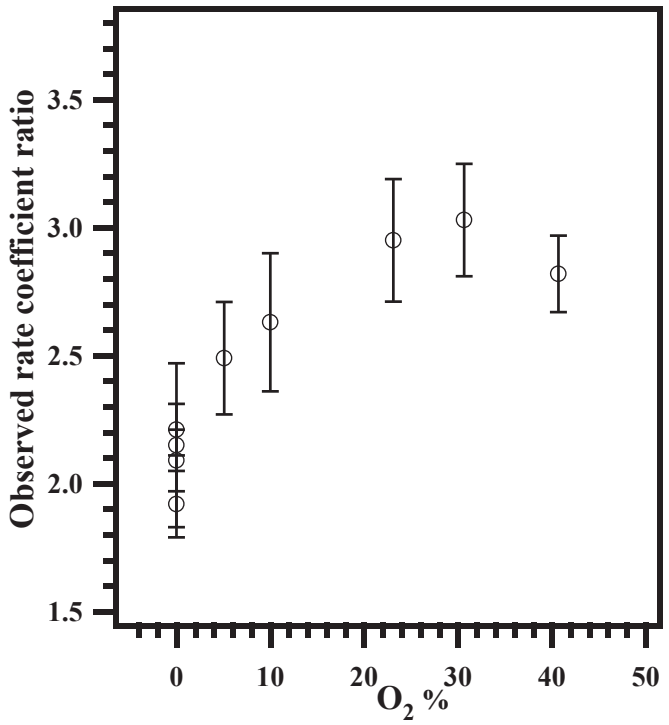

Fig. 4. Variation of the observed rate coefficient ratio of limonene, with reference to that of 1-pentene at different partial pressures of oxygen.

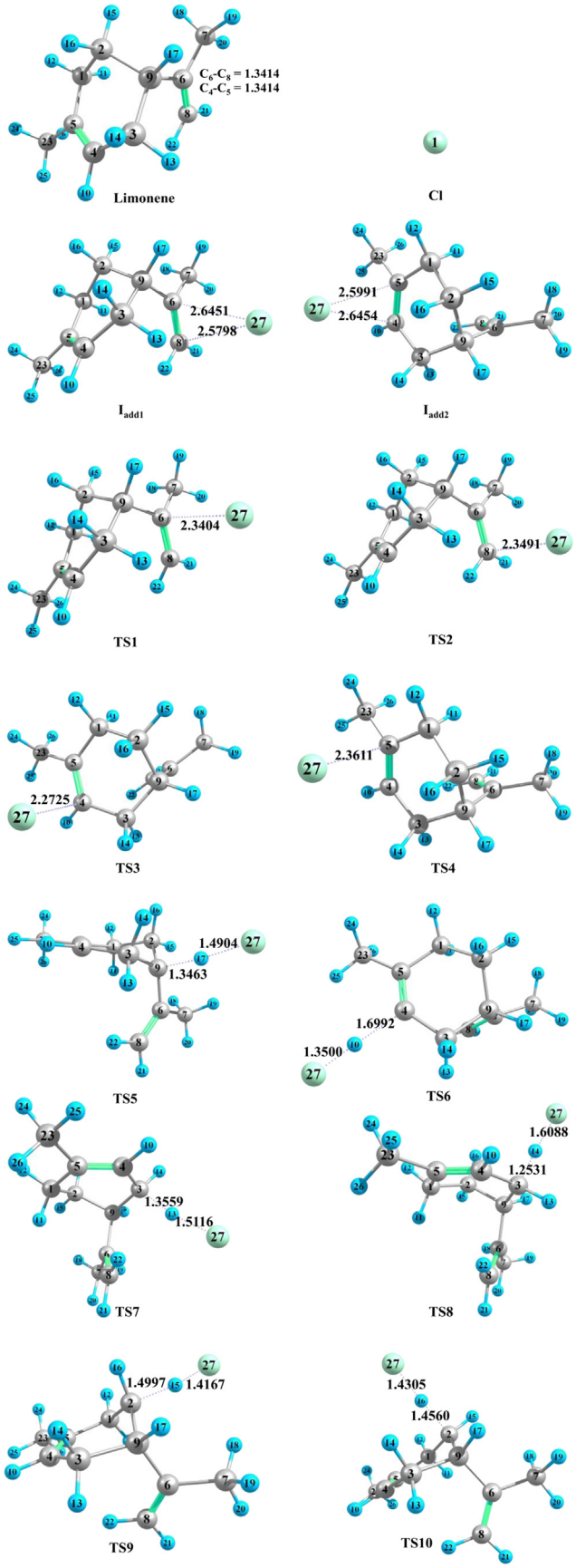

Fig. 5. Geometries of the reactants, intermediates (I_{adds}), transition states (TSs), and products optimized at MP2(FULL)/6-31G(d) level of theory. Sky blue represents hydrogen, black represents carbon, and light green represents chlorine atoms in the structures. The bond lengths (Å) given on the structures are obtained at MP2(FULL)/6-31G(d) level of theory. (For interpretation of the references to color in this figure legend, the reader is referred to the web version of this article.)

and 350 K, and the obtained rate coefficients are given in Table 2. Each set of experiments were repeated at least twice. For each experiment, slope and errors were obtained from the linear least-square fitting of the data. The quoted errors for the rate coefficients obtained using 1,3-butadiene and n-nonane as references are two least-squares standard deviations and include uncertainties in the rate coefficients of $k_{1,3\text{-butadiene}}$ (Ragains and Finlayson-Pitts, 1997) and $k_{\text{n-nonane}}$ (Aschmann and Atkinson, 1995). Whereas, the quoted errors for the rate coefficients obtained using 1-pentene as a reference compound are two least-squares standard deviations and do not include uncertainties in the rate coefficients of $k_{1\text{-pentene}}$ (Coquet and Ariya, 2000). Fig. 2 shows typical plots of obtained data for the reaction of Cl atoms with limonene at 278, 298, 320, and 340 K. The maximum deviation in the measured data at any given temperature was 10%. We have included the error limits ($\pm 2\sigma$) in Figs. 1 and 2. For each point in Figs. 1 and 2, the error limits indicates the systematic errors such as measurement in the concentrations and temperature. The Arrhenius plot of the reaction is shown in Fig. 3. The rate coefficients were found to be increasing with decrease in temperature, showing a negative temperature dependence. The linear least-squares fit of the measured rate coefficients between 278 and 350 K resulting an Arrhenius expression: k_{limonene} (278–350 K) = $(9.75 \pm 4.1) \times 10^{-11}$ exp[(655 ± 133)/T] cm^3 molecule^{-1} s^{-1}. The quoted uncertainties in the Arrhenius expression are the 2σ (95% confidence limits) precision from the statistical errors due to the linear least-squares fit of the rate coefficients data obtained between the temperature range of 278 and 350 K. The negative temperature dependence on rate coefficients can be explained by reversible formation of a pre-reactive complex between Cl atom and limonene along the reaction coordinate. The rate coefficient for the title reaction obtained at 298 K with 1-pentene as a reference compound to be $(9.81 \pm 1.17) \times 10^{-10}$ cm^3 molecule^{-1} s^{-1} which is in reasonably good agreement (~10% deviation) with the rate coefficient $[(8.82 \pm 0.58) \times 10^{-10}$ cm^3 molecule^{-1} $\text{s}^{-1}]$ obtained using n-nonane as a reference compound. However, the rate coefficients obtained at 298 K using n-nonane and 1-pentene as reference compounds are ~20–25 % higher than the one obtained using 1,3-butadine as a reference compound $[(7.31 \pm 1.81) \times 10^{-10}$ cm^3 molecule^{-1} $\text{s}^{-1}]$ and the literature value $[(6.4 \pm 0.8) \times 10^{-10}$ cm^3 molecule^{-1} $\text{s}^{-1}]$ reported by Finlayson-Pitts et al. (1999). The discrepancies between these results may be due to the errors associated with the reference reaction's rate coefficients used in the measurements. Therefore, we prefer to quote final value for the rate coefficient at 298 K to be $(8.65 \pm 2.44) \times 10^{-10}$ cm^3 molecule^{-1} s^{-1} which is average value of all three rate coefficients using different reference compounds. Similarly, we quoted the final values of the rate coefficients at various temperatures by taking the averages of the rate coefficients obtained using n-nonane and 1-pentene as reference compounds (Table 2).

We cannot rule out the possibility of the secondary chemistry that may be initiated by the radical produced after association and thereby contribute to the secondary losses of the reactant. A good way of confirming this effect is via scavenging the radicals by adding oxygen. We have carried out the experiments in the presence of different concentrations of oxygen at 298 K by using 1-pentene as a reference compound. A systematic increase in the relative rate ratio up to 30% of oxygen was observed, as shown in Fig. 4 and which means that the rate coefficient is gradually

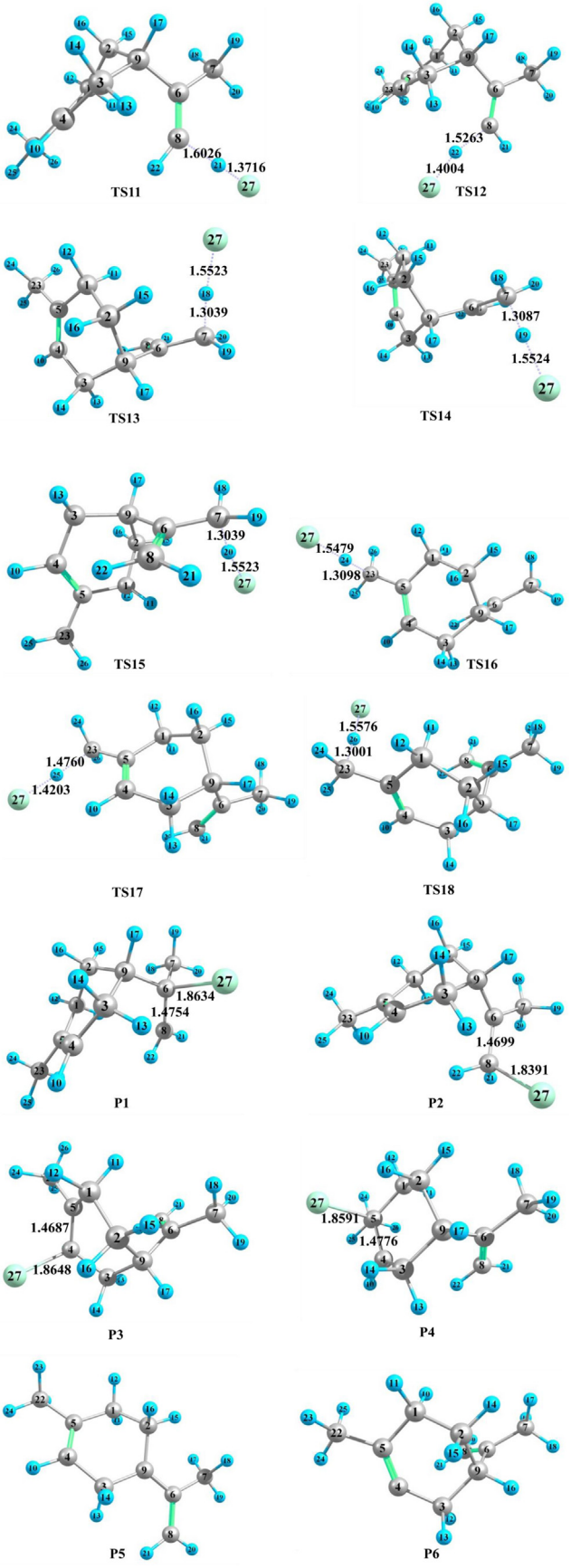

Fig. 5. (*continued*).

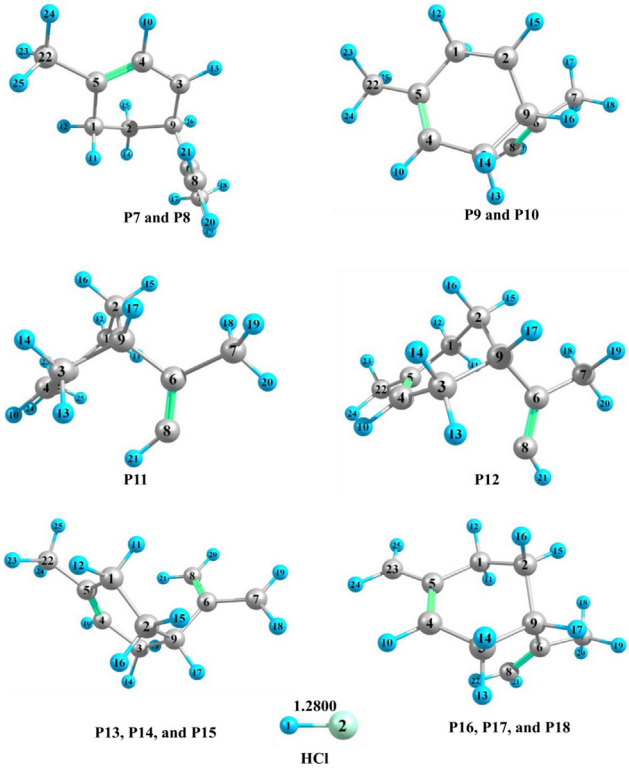

Fig. 5. (*continued*).

becoming higher as the O_2 concentration is increased. However, at the lowest O_2 levels, the measured rate coefficients are in good agreement with the rate coefficient reported by Finlayson-Pitts et al. (1999) and which is quite surprising to us. This shows that, seems like there are large uncertainties in the measurement of reference reaction's rate coefficient reported by Coquet and Ariya (2000).

3.2. Electronic structures and energetics

Geometries of the reactants, intermediates (I_{adds}), TSs, and products were optimized at MP2(FULL) level of theory using 6-31G(d) basis set. Fig. 5 shows the calculated optimized geometries of reactants, intermediates (I_{adds}), TSs, and products at the MP2(FULL)/6-31G(d) level of theory. Addition of Cl atom at C_6 and C_8 carbons of the C_6═C_8 bond of limonene lead to the formation of adducts P1 (primary radical) and P2 (tertiary radical) via TS1 and TS2 respectively. Similarly, Cl additions at C_4 and C_5 carbons of the C_4═C_5 bond leads to the formation of adducts P3 (tertiary radical) and P4 (secondary radical) via TS3 and TS4 respectively. When the addition take place between Cl atoms and the double bonds of limonene, they form a stable molecular complex (symmetrically bridged structure; I_{add}) before proceeding to transition state (asymmetrically bridged structure) and then form corresponding adduct radicals. Due to these additions, C_6═C_8 and C_4═C_5 bond lengths in limonene are elongated from 1.3 Å to 1.5 Å. In addition to the addition reactions, hydrogen abstraction reactions are also possible in limonene by Cl atom from different carbons sites of limonene, which leads to the formation of products P5 to P18 and HCl molecule via transition states TS5 to TS18, respectively. TS5 correspond to the abstraction of hydrogen atom from the tertiary carbon atom (C_9) of isopropenyl group, TS6 correspond to the abstraction of hydrogen from –CH═ group (C_4), TS7 to TS10

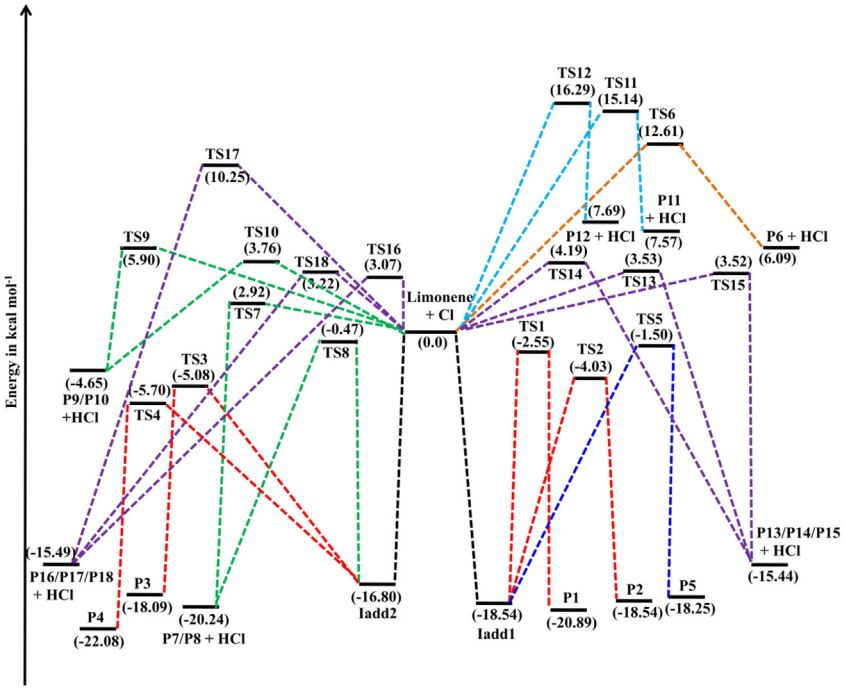

Fig. 6. Energy level diagram for the reaction through all the transition states obtained at G3(MP2) level of theory. The energies are given in the units of kcal mol^{-1}. Red dotted lines: addition pathways, blue dotted lines: tertiary hydrogen abstraction pathway, light blue dotted lines: =CH_2 hydrogen abstraction pathways, orange dotted lines: –CH= hydrogen abstraction pathway, green dotted lines: secondary hydrogen abstraction pathways, purple dotted lines: primary hydrogen abstraction pathways. (For interpretation of the references to color in this figure legend, the reader is referred to the web version of this article.)

correspond to the abstraction of hydrogen from two secondary carbon atoms (C_2 and C_3), TS11 and TS12 correspond to the abstraction of hydrogen from =CH_2 group (C_8), and TS13 to TS18 correspond to abstraction of hydrogen from two methyl (primary carbons) groups (C_7 and C_{23}) of limonene. However, the transition states corresponding to the abstraction of hydrogen from one secondary carbon atom (C_1) could not be located. In the transition states of hydrogen abstractions from tertiary carbon (TS5) atom of isopropenyl group, –CH] group (TS6), =CH_2 group (TS11 and TS12), and secondary carbon atoms (TS7, TS9, and TS10 except TS8), the elongation of the breaking C–H bonds are greater than that of the forming H–Cl bonds indicating that the transition states are product-like and the reactions will proceed via late transition states. However, in case of the transition states of hydrogen abstraction from two methyl (primary carbons) groups (TS13, TS14, TS15, TS16, and TS18 except TS17) the elongation of forming H–Cl bonds are larger than that of breaking C–H bonds indicating that the transition states are reactant-like and the reactions will proceed via early transition state. The elongation of the bond lengths between the C–H and H–Cl bonds of reactants and TSs at MP2(FULL)/6-31G(d) level of the theory are given in the Supporting Information (Table S-I). The vibrational frequencies and structural parameters of reactants, intermediates (I_{adds}), transition states (TSs), and products in limonene + Cl reaction are given in the Supporting Information (Tables S-II and S-III). The vibrational frequencies used in the calculation of the partition functions, which are required to compute the rate coefficient were not scaled in the present study.

To obtain more accurate energies and barrier heights, the energies were refined by using a potentially high-level *ab initio* method G3(MP2) (Curtiss et al., 1999) based on MP2(FULL)/6-31G(d) optimized geometries. The schematic potential energy surfaces (PESs) of addition and abstraction channels obtained at G3(MP2) level of theory are depicted in Fig. 6. The barriers energies for additions channels (TS1–TS4) are found to be negative and the barriers for abstractions channels (TS5–TS20) are much higher

Table 3
The reaction enthalpies ($\Delta H^\circ_{298\ K}$, kcal mol^{-1}), free energies ($\Delta G^\circ_{298\ K}$, kcal mol^{-1}) and entropies ($\Delta S^\circ_{298\ K}$, cal mol^{-1} K^{-1}) are calculated at G3(MP2) level of theory.

Addition/abstraction site (TS)	ΔG°	ΔH°	ΔS°
C_6 (TS1)	−10.09	−18.98	−29.82
C_8 (TS2)	−13.81	−21.23	−24.88
C_4 (TS3)	−11.24	−18.35	−23.86
C_5 (TS4)	−14.10	−22.62	−28.59
C_9 (TS5)	−20.28	−17.44	9.55
C_4 (TS6)	4.22	6.73	8.40
C_3 (TS7/TS8)	−22.21	−19.49	9.11
C_2 (TS9/TS10)	−6.69	−3.85	9.52
C_8 (TS11)	5.67	8.23	8.58
C_8 (TS12)	5.65	8.38	9.14
C_7 (TS13/TS14/TS15)	−16.93	−14.93	6.68
C_{23} (TS16/TS17/TS18)	−17.15	−14.99	7.24

Table 4
Rate coefficients (cm^3 molecule^{-1} s^{-1}) for limonene + Cl reaction in the temperature range of 275 and 400 K at G3(MP2) level of theory.

T (K)	TST	TST/Wigner	TST/Eck_Sym	Present exptl. and literature values
275	3.58×10^{-09}	3.99×10^{-09}	4.00×10^{-09}	[a] $(7.31 \pm 1.81) \times 10^{-10}$
298	1.82×10^{-09}	1.99×10^{-09}	2.00×10^{-09}	[b] $(9.16 \pm 2.67) \times 10^{-10}$
300	1.72×10^{-09}	1.89×10^{-09}	1.89×10^{-09}	[c] $(8.82 \pm 0.58) \times 10^{-10}$
325	9.42×10^{-10}	1.02×10^{-09}	1.02×10^{-09}	[d] $(9.81 \pm 1.17) \times 10^{-10}$
350	5.67×10^{-10}	6.08×10^{-10}	6.09×10^{-10}	(present experiment)
375	3.69×10^{-10}	3.92×10^{-10}	3.93×10^{-10}	[e] $(6.4 \pm 0.8) \times 10^{-10}$
400	2.55×10^{-10}	2.70×10^{-10}	2.70×10^{-10}	(Finlayson-Pitts et al., 1999)

[a] 298 K in N_2 (1,3-butadiene as a reference compound).
[b] 298 K in Air (1,3-butadiene as a reference compound).
[c] 298 K in N_2 (n-nonane as a reference compound).
[d] 298 K in N_2 (1-pentene as a reference compound).
[e] 298 K (relative-rate technique).

Table 5
Rate coefficients of the various channels for limonene + Cl reaction in the temperature range of 275 and 400 K at G3(MP2) level of theory.

T (K)	Rate coefficients (10^{-10} cm^3 molecule^{-1} s^{-1})														
	TST					TST/Wigner					TST/Eck_Sym				
	k_{TS1}	k_{TS2}	k_{TS3}	k_{TS4}	k_{TS5}	k_{TS1}	k_{TS2}	k_{TS3}	k_{TS4}	k_{TS5}	k_{TS1}	k_{TS2}	k_{TS3}	k_{TS4}	k_{TS5}
275	0.03	2.30	16.9	16.6	0.03	0.04	2.53	18.8	18.4	0.06	0.04	2.54	18.9	18.4	0.06
298	0.02	1.40	8.91	7.82	0.03	0.03	1.52	9.81	8.54	0.05	0.03	1.53	9.84	8.57	0.05
300	0.02	1.35	8.47	7.37	0.03	0.03	1.46	9.31	8.04	0.05	0.03	1.47	9.34	8.06	0.05
325	0.02	0.86	4.77	3.74	0.02	0.02	0.93	5.18	4.03	0.04	0.02	0.93	5.19	4.04	0.04
350	0.01	0.59	2.94	2.10	0.02	0.02	0.63	3.15	2.25	0.04	0.02	0.63	3.16	2.25	0.04
375	0.01	0.43	1.94	1.29	0.02	0.01	0.45	2.06	1.36	0.03	0.01	0.45	2.07	1.36	0.03
400	0.01	0.33	1.35	0.84	0.02	0.01	0.34	1.43	0.88	0.03	0.01	0.34	1.43	0.89	0.03

(Fig. 6) than the addition channels; which suggest that the contribution of abstraction reactions to the total reaction are negligible. It is clear from Fig. 6 that, abstraction of hydrogen from −CH═ group (TS6) and ═CH_2 group (TS11 and TS12) are endothermic in nature which shows that these reaction pathways are thermodynamically unfavorable.

The standard enthalpy (ΔH°_{298K}), free energy (ΔG°_{298K}), and entropy change (ΔS°_{298K}) of the reaction through all the addition and H-abstraction reaction channels were calculated at G3(MP2) level of theory and are given in Table 3. All addition and abstraction channels are found to be exothermic ($\Delta H^\circ_{298K} < 0$) and exergonic ($\Delta G^\circ_{298K} < 0$) reactions except hydrogen abstraction from −CH═ group (C_4) and ═CH_2 group (C_8) which are endothermic ($\Delta H^\circ_{298K} > 0$) and endergonic ($\Delta G^\circ_{298K} > 0$) reactions. The formation of abstraction products seems to be thermodynamically more favorable than addition products except the products obtained from C_2 (TS9/TS10) carbon. Among all addition reactions, addition at C_5 (TS4) is thermodynamically most favorable pathway followed by additions at C_8 (TS2), C_4 (TS3), and C_6 (TS1). Whereas, among all abstraction reactions, H-abstraction from ═CH_2 (C_8) and ═CH− (C_4) groups are thermodynamically unfavorable and H-abstraction from one of the secondary carbon atom (C_3) is the most favorable reaction pathway followed by H-abstractions from tertiary carbon atom (C_9) of isopropenyl group, primary carbon atoms (C_7 and C_{23}), and then other secondary carbon atom (C_2).

3.3. Kinetic analysis

As mentioned above, the barrier energies for abstraction channels are too high when compared to addition channels and their contributions to the total reaction are negligible. Therefore, rate coefficients were calculated for only addition channels (TS1−TS4) and tertiary H-abstraction channel (TS5) which has lowest barrier among all abstraction channels, using the conventional transition state theory (CTST) in combination with Wigner's and Eckart's symmetrical tunneling methods in the temperature range of 275−400 K. The barrier energies obtained at G3(MP2) level of theory were used in TST calculations. The calculated TST, TST/Wigner, and TST/Eck_Sym rate coefficients (in cm^3 molecule^{-1} s^{-1}) for the limonene + Cl reaction in the temperature range of 275−400 K along with the present experimental and the only available reported value at room temperature are given in Table 4. The rate coefficients obtained using Wigner's and Eckart's methods are found to be almost similar. It is clear from Table 4 that, the tunneling effect is small at lower temperatures and is observed to be negligible as the temperature rises. For example, the $k_{TST/Wigner}/k_{TST}$ and $k_{TST/Eck\_Sym}/k_{TST}$ ratios are 1.11 and 1.12 at 275 K and 1.06 at 400 K. The rate coefficients (in cm^3 molecule^{-1} s^{-1}) for the limonene + Cl reaction (Table 4) are obtained from the sum of the calculated individual rate coefficients ($k = k_{TS1} + k_{TS2} + k_{TS3} + k_{TS4} + k_{TS5}$). The rate coefficients of the various addition channels (k_{TS1} to k_{TS4}) and tertiary H-abstraction channel (k_{TS5}) for the limonene + Cl reaction over the temperature range of 275−400 K at G3(MP2) level of theory are given in Table 5. It is clear from Table 5 that, the rate coefficients for tertiary H-abstraction channel (k_{TS5}) are negligible when compared with the total rate coefficient obtained for limonene + Cl reaction in the temperature range of 275−400 K. The rate coefficients obtained in our calculations are approximately two to three times higher than our experimentally measured rate coefficient and reported literature value (Finlayson-Pitts et al., 1999) at room temperature using relative rate technique. However, at ~350 K, the rate coefficient obtained in our calculations (6.09×10^{-10} cm^3 molecule^{-1} s^{-1}) is in very good agreement with the rate coefficient measured in our experiment ($(6.13 \pm 0.63) \times 10^{-10}$ cm^3 molecule^{-1} s^{-1} (Tables 4 and 2). It should be noted here that, the rate coefficients given in Tables 4 and 5 are too high at low temperatures (at 278 K, ~4 times higher than the present experimental investigations). Even at room temperature, the quoted rate coefficients are ~2 times higher than the collision rate limit ~8×10^{-10} cm^3 moecule^{-1} s^{-1}, implying that the reaction proceeds faster than a collision! This could only happen when ions

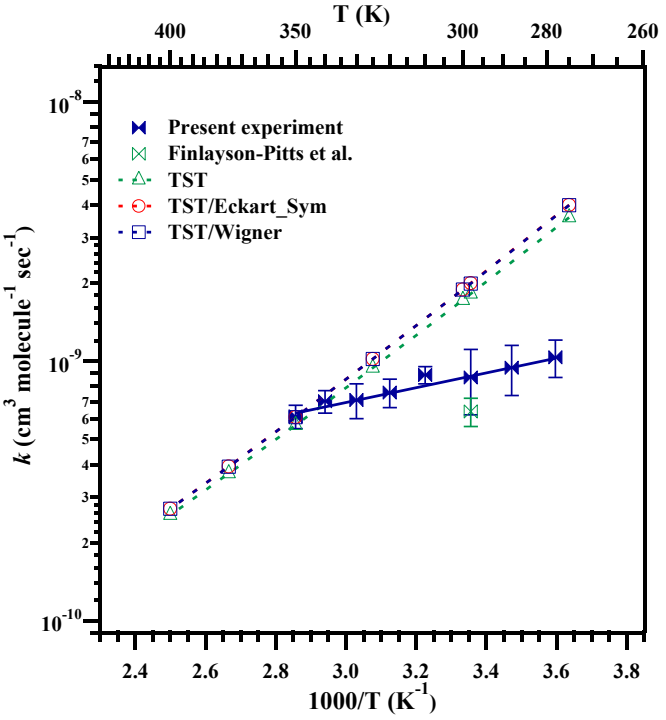

Fig. 7. Arrhenius plot of the rate coefficient data obtained for the limonene + Cl reaction over the temperature range of 275−400 K. The data are identified by different symbols defined in the Figure.

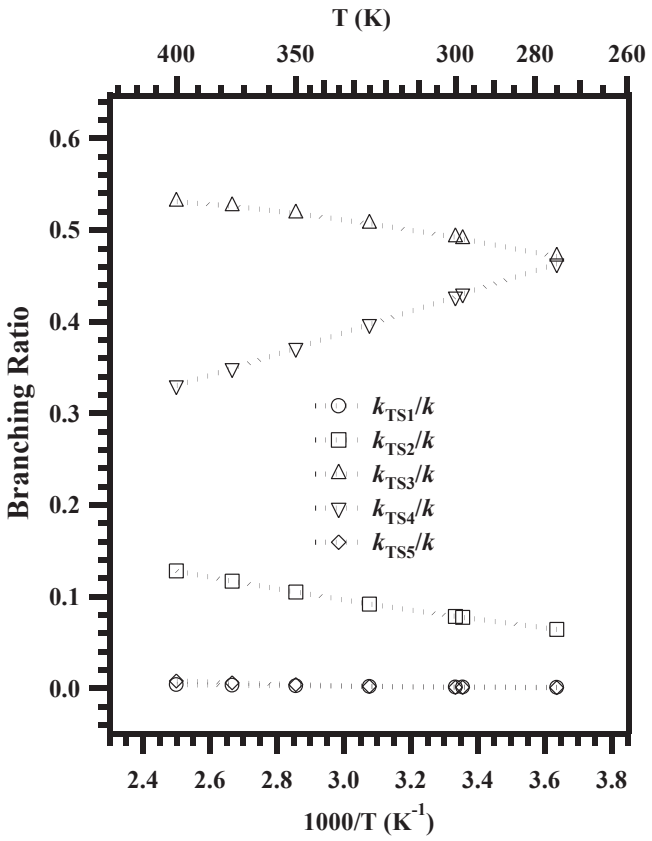

Fig. 8. Calculated branching ratios of k_{TS1}, k_{TS2}, k_{TS3}, k_{TS4}, and k_{TS5} to the total rate coefficient for limonene + Cl reaction over the temperature range of 275–400 K.

are involved, which is not the case in the studied reaction. The possible reason for this behavior could be the intrinsic drawback of the methodology/theory used to compute these rate coefficients. In the present case (i.e., the reaction of Cl atom with limonene), the barrier energies calculated using G3(MP2) theory for all addition channels and tertiary abstraction channel are in the range of −5.7 to −1.5 kcal mol^{-1}. For these barrierless reactions, the variational effects on the rate coefficient may expected to be significant. When we have tried to perform the canonical variational transition state theory (CVT) calculations for all these barrierless reactions to get meaningful rate coefficients (well below the collision limits), we could not find out correct intrinsic reaction coordinates (IRCs), due to convergence problems. Therefore, we are bound to carry out rate coefficient calculations using conventional transition state theory (CTST) only and reported the CTST calculations in the present investigations.

The Arrhenius plot of the rate coefficient data obtained using TST, TST/Wigner, and TST/Eck_Sym calculations in the temperature range of 275–400 K along with the present experimentally measured rate coefficients obtained in the temperature range of 278–350 K and the available reported rate coefficient at 298 K are depicted in Fig. 7. It is obvious from the Figure that, the theoretically calculated rate coefficients exhibit a strong negative temperature dependence while the experimentally measured rate coefficients are showing slight negative temperature dependence for the limonene + Cl reaction over the studied temperature range and the data were fit by linear least-squares fit, and the obtained Arrhenius expressions are (in cm^3 $molecule^{-1}$ s^{-1}):

$$k_{\text{Experiment}}(278-350) = (9.75\pm4.1)\times10^{-11}\exp[(655\pm133)/T]$$

$$k_{\text{TST}}(275-400\ \text{K}) = (7.92\pm0.82)\times10^{-13}\exp[(2310\pm34)/\text{T}]$$

$$k_{\text{TST/Wigner}} = k_{\text{TST/Eck\_Sym}}(275-400\ \text{K}) = (7.07\pm0.73)\times10^{-13}\exp[(2370\pm34)/T]$$

The calculated pre-exponential factors are nearly two orders of magnitude lower than the pre-exponential factor obtained in our measurements. On the other hand, the calculated activation energy (E_a) is ~−4.6 kcal mol^{-1}, which is nearly three times larger than the experimentally measured E_a (−1.3 kcal mol^{-1}) obtained in our measurements. The pre-exponential factors depends mainly on how best the partition functions of both the transition state and reactants are estimated, which in turn depends on the vibrational frequencies obtained using the chosen theory for these calculations. One more possible reason for the discrepancy between experimental and theoretical kinetic data may be due to the uncertainty associated with the reference reaction rate coefficients values used in the experimental measurements.

The branching ratios of individual addition channels ($k_{TS1}/k - k_{TS4}/k$) and tertiary hydrogen abstraction channel (k_{TS5}/k) over the whole temperature range of 275–400 K are given in Fig. 8. As seen in Fig. 8, additions of Cl atom at C_4 and C_5 carbons are the major contributors to the total rate coefficients, whereas, addition at C_8 carbon is the minor contributor, and addition at C_6 and H-abstraction from tertiary carbon (C_9) is the negligible contributor to the total rate coefficient in the studied temperature range. For example, k_{TS2}/k (C_8), k_{TS3}/k (C_4), and k_{TS4}/k (C_5) ratios are 0.06, 0.47, and 0.46 at 275 K, 0.08, 0.49, and 0.43 at 298 K, and 0.13, 0.53, and 0.33 at 400 K, respectively. These values suggest that the contributions of Cl atom additions at C_8 and C_4 carbons to the total rate coefficients increases with increase in temperature over the studied temperate range, while the contribution of Cl atom addition at C_5 carbon decreases with increase in temperature.

4. Atmospheric implications

Atmospheric degradation of limonene mainly happens via its reactions with tropospheric oxidants like OH and NO_3 radicals, O_3, and possibly Cl atoms. The Atmospheric lifetime (τ) of limonene due to its reaction with Cl atom was estimated using equation.

Table 6
Calculated atmospheric lifetimes of limonene due to its reaction with Cl atoms and OH radicals.

τ_{Cl} (days)[a]				τ_{Cl} (hours)[b]				τ_{OH} (hours)[c]
Present experiment	TST	TST/Wigner	TST/Eck_Sym	Present experiment	TST	TST/Wigner	TST/Eck_Sym	Gill and Hites (2002)
14.3	6.1	5.5	5.5	2.6	1.1	1.0	1.0	1.7

[a] Upper limit chlorine atom average concentration, [Cl] = 10^3 atoms cm^{-3} (Singh et al., 1996).
[b] Coastal and marine boundary layer, [Cl] = 1.3×10^5 atoms cm^{-3} (Spicer et al., 1998).
[c] Hydroxyl radical average concentration, [OH] = 1.0×10^6 radicals cm^{-3} (Prinn et al., 1995).

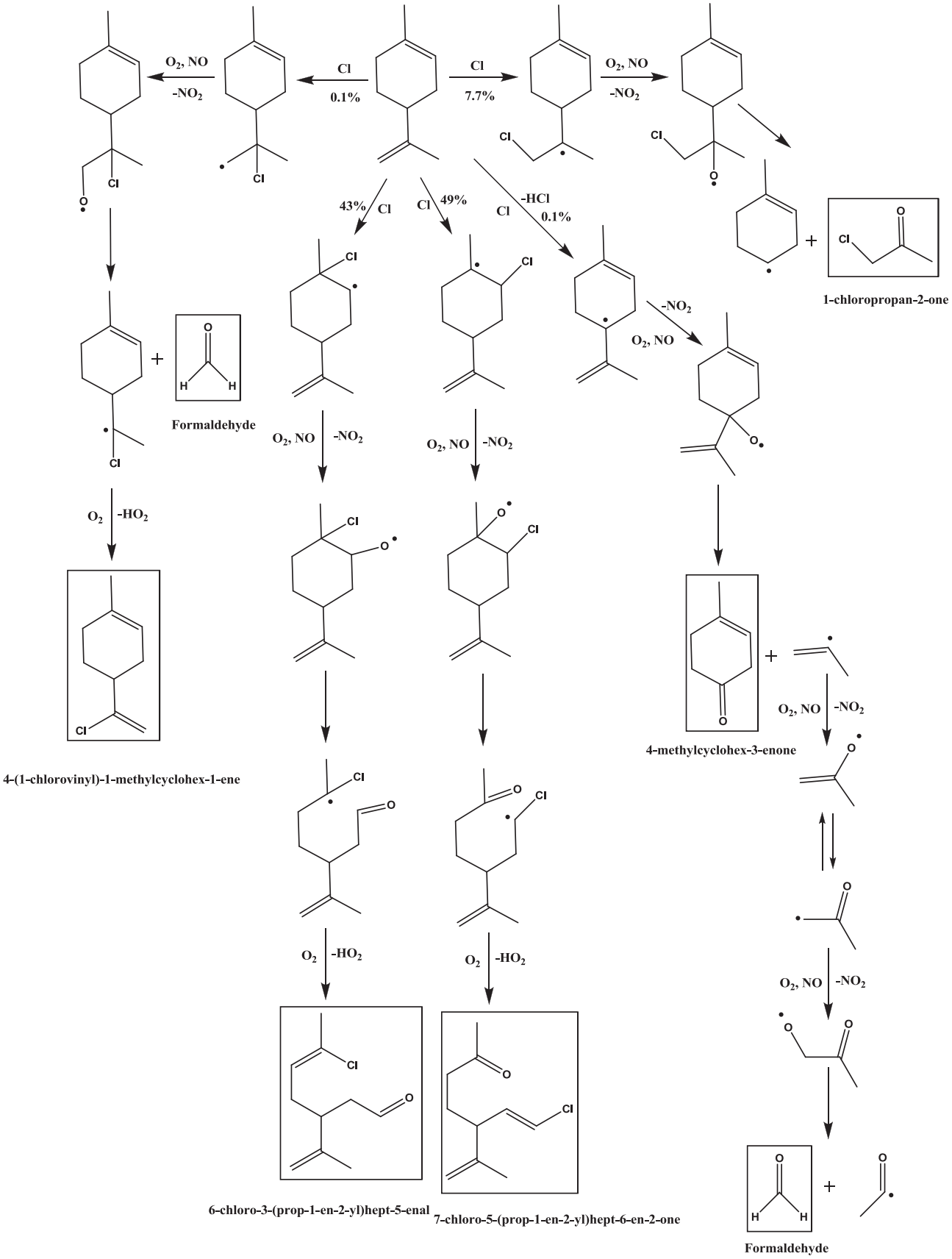

Fig. 9. Proposed Cl initiated atmospheric degradation mechanism for limonene in the NO-rich environment. Compounds in the boxes are stable products.

$$\tau = 1/k_{Cl}[Cl] \quad (4)$$

where k_{Cl} is the rate coefficient of limonene at 298 K with Cl atoms obtained in present investigation and [Cl] is the global average concentration of the Cl atoms (1.0×10^3 atom cm^{-3}) reported by Singh et al. (1996) and Wingenter et al. (1999). In coastal and marine boundary layer, Spicer et al. (1998) observed a high Cl concentration of 1.3×10^5 atom cm^{-3}, which has also been used in the estimation of atmospheric lifetimes under these specific conditions. Table 6 shows the calculated atmospheric lifetimes of limonene due to reactions with Cl atoms. By using the rate coefficient (1.61×10^{-10} cm^3 $molecule^{-1}$ s^{-1}) of limonene due to reaction with OH radicals (Gill and Hites, 2002), the OH-driven atmospheric lifetime of limonene was calculated and included in Table 6 for comparison.

The global atmospheric lifetime for reaction of limonene with OH radicals is 1.7 h. For the reaction with Cl, using a Cl average concentration of 10^3 atom cm^{-3}, global lifetime of limonene was found to be 6–14 days (when the rate coefficients obtained by all methods are considered). Using a higher Cl atom concentration in coastal and marine areas (1.3×10^5 atom cm^{-3}), the atmospheric lifetime of the limonene due to the Cl-reaction is around 1–2.6 h. The lifetimes data indicates that the removal of limonene from Earth's atmosphere mainly due to its reaction with OH radicals; nevertheless, in coastal and marine areas, where the concentrations of Cl atoms are sufficiently high, reaction of this compound with Cl atoms can compete with the OH radicals reaction.

Fig. 9 shows the reaction mechanism proposed for the oxidation of limonene with Cl atoms in a nitrogen-rich environments. The reaction of limonene with Cl atoms will go through mainly via addition on two unsaturated carbon–carbon bonds and leads to the formation of corresponding chloroalkyl radicals. These radicals react with O_2 to form corresponding peroxy radicals and followed by reaction with NO to form corresponding alkoxy radicals. These alkoxy radicals undergo Unimolecular decomposition to form stable products like formaldehyde, 4-(1-chlorovinyl)-1-methylcyclohex-1-ene, 1-chloropropan-2-one, 6-chloro-3-(prop-1-en-2-yl)hept-5-enal, and 7-chloro-5-(prop-1-en-2-yl)hept-6-en-2-one. Cl atom also can abstract hydrogen from the tertiary carbon atom of isopropenyl group of limonene to form corresponding alkyl radical. This radical react with O_2 and NO to form corresponding alkoxy radical and then decomposes to stable products such as 4-methylcyclohex-3-enone and formaldehyde. The resulting products may further be degraded via their reactions with various oxidizing species in the atmosphere and which leads to the formation of ozone in the troposphere.

5. Conclusions

In this paper, the kinetics of the reaction of limonene with Cl atoms was investigated using relative technique and *ab initio* methods. This work represents the first kinetic study of the reaction of Cl atoms with limonene as a function of temperature. Both experimentally measured and theoretically calculated rate coefficients have exhibited negative temperature dependence. The PES of the title reaction shows that the addition channels are only contributors to the total reaction and H-abstraction channels can be neglected completely. The atmospheric lifetime of limonene was calculated and concluded that the reaction with chlorine atoms can provide an effective tropospheric loss pathway in the marine boundary layer and in coastal urban areas (where Cl atoms concentration is high).

Acknowledgments

The authors thank Professor Donald G. Truhlar and his group for providing the POLYRATE 2008 and GAUSSRATE 2009A programs. Also the authors thank the High Performance Computing centre and Mr. V. Ravichandran for providing computer resources. BR thanks the BRNS, Government of India (Sanction No. 2012/37C/22/BRNS) for the research funding.

Appendix A. Supplementary data

Supplementary data related to this article can be found at http://dx.doi.org/10.1016/j.atmosenv.2014.09.066.

References

Aschmann, S.M., Atkinson, R., 1995. Rate constants for the gas-phase reactions of alkanes with Cl atoms at 296 ± 2 K. Int. J. Chem. Kinet. 27, 613–622.
Bonsang, B., Polle, C., Lambert, G., 1992. Evidence for marine production of isoprene. Geophys. Res. Lett. 19, 1129–1132.
Chase Jr., M.W., 1998. NIST-JANAF thermochemical tables. fourth ed. J. Phys. Chem. Ref. Data 9, 1298.
Coquet, S., Ariya, P.A., 2000. Kinetics of the gas-phase reactions of Cl atom with selected C_2–C_5 unsaturated hydrocarbons at 283 < T < 323 K. Int. J. Chem. Kinet. 32, 478–484.
Curtiss, L.A., Redfern, P.C., Raghavachari, K., Rassolov, V., Pople, J.A., 1999. Gaussian-3 theory using reduced Møller-Plesset order. J. Chem. Phys. 110, 4703–4709.
Dash, M.R., Rajakumar, B., 2012. Abstraction kinetics of H-Atom by OH radical from pinonaldehyde ($C_{10}H_{16}O_2$): ab initio and transition-state theory calculations. J. Phys. Chem. A 116, 5856–5866.
Dash, M.R., Rajakumar, B., 2013. Experimental and theoretical rate coefficients for the gas phase reaction of β-pinene with OH radical. Atmos. Environ. 79, 161–171.
Dash, M.R., Balaganesh, M., Rajakumar, B., 2013. Rate coefficients for the gas-phase reaction of OH radical with α-pinene: an experimental and computational study. Mol. Phys. http://dx.doi.org/10.1080/00268976.2013.840395.
Dobis, O., Benson, S.W., 1991. Temperature coefficients of the rates of chlorine atom reactions with C_2H_6, C_2H_5, and C_2H_4. The rates of disproportionation and recombination of ethyl radicals. J. Am. Chem. Soc. 113, 6377–6386.
Eckart, C., 1930. The penetration of potential barrier by electrons. Phys. Rev. 35, 1303–1309.
Finlayson-Pitts, B.J., Keoshian, C.J., Buehler, B., Ezell, A.A., 1999. Kinetics of reaction of chlorine atoms with some biogenic organics. Int. J. Chem. Kinet. 31, 491–499.
Frisch, M.J., Trucks, G.W., Schlegel, H.B., Scuseria, G.E., Robb, M.A., Cheeseman, J.R., Scalmani, G., Barone, V., Mennucci, B., Petersson, G.A., et al., 2010. Gaussian 09, Revision B.01. Gaussian, Inc., Wallingford, CT, USA.
George, C., Behnke, W., Zetzsch, C., 2010. Radicals in the atmosphere: a changing world! ChemPhysChem 11, 3059–3062.
Gill, K.J., Hites, R.A., 2002. Rate constants for the gas-phase reactions of the hydroxyl radical with isoprene, α- and β-pinene, and limonene as a function of temperature. J. Phys. Chem. A 106, 2538–2544.
Glasow, R.V., 2010. Atmospheric chemistry: wider role for airborne chlorine. Nature 464, 168–169.
Johnston, H.S., Heicklen, J., 1962. Tunneling corrections for unsymmetrical Eckart potential energy barriers. J. Phys. Chem. 66, 532–533.
Kaiser, E.W., Wallington, T.J., 1996. Kinetics of the reactions of chlorine atoms with C_2H_4 (k_1) and C_2H_2(k_2): a determination of $\Delta H_{f,298}^{\circ}$ for C_2H_3. J. Phys. Chem. 100, 4111–4119.
Lee, F.S.C., Rowland, F.S., 1977. Thermal chlorine-38 atom reactions with ethylene. J. Phys. Chem. 81, 1235–1239.
Lewis, R.S., Sander, S.P., Wagner, S., Walson, R.T., 1980. Temperature-dependent rate constants for the reaction of ground-state chlorine with simple alkanes. J. Phys. Chem. 84, 2009–2015.
McKay, W.A., Turner, M.F., Jones, B.M.R., Halliwell, C.M., 1996. Emissions of hydrocarbons from marine phytoplankton—some results from controlled laboratory experiments. Atmos. Environ. 30, 2583–2593.
Milne, P.J., Reimer, D.D., Zika, R.G., Brand, L.E., 1995. Measurement of vertical distribution of isoprene in surface seawater, its chemical fate, and its emission from several phytoplankton monocultures. Mar. Chem. 48, 237–244.
Moore, R.M., Oram, D.E., Penkett, S.A., 1994. Production of isoprene by marine phytoplankton cultures. Geophys. Res. Lett. 21, 2507–2510.
Osthoff, H.D., Roberts, J.M., Ravishankara, A.R., Williams, E.J., Lerner, B.M., Sommariva, R., Bates, T.S., Coffman, D., Quinn, P.K., Dibb, J.E., et al., 2008. High levels of nitryl chloride in the polluted subtropical marine boundary layer. Nat. Geosci. 1, 324–328.
Parmar, S.S., Benson, S.W., 1988. Kinetics of the reaction chlorine atom + ethylene.dblharw. vinyl + hydrogen chloride: heat of formation of the vinyl radical. J. Phys. Chem. 92, 2652–2657.

Pilgrim, J.S., Taatjes, C.A., 1997. Infrared absorption probing of the Cl + C_2H_4 reaction: direct measurement of Arrhenius parameters for hydrogen abstraction. J. Phys. Chem. A 101, 4172–4177.
Prinn, R.G., Weiss, R.F., Millar, B., Huaung, J., Alyea, F.N., Cunnold, D.M., Fraser, P.J., Hartley, D.E., Simmonds, P.G., 1995. Atmospheric trends and lifetime of CH_3CCl_3 and global OH concentrations. Science 269, 187–192.
Ragains, M.L., Finlayson-Pitts, B.J., 1997. Kinetics and mechanism of the reaction of Cl atoms with 2-methyl-1,3-butadiene (isoprene) at 298 K. J. Phys. Chem. A 101, 1509–1517.
Ratte, M., Bujok, O., Spitzy, A., Rudolph, J., 1998. Photochemical alkene formation in seawater from dissolved organic carbon: results from laboratory experiments. J. Geophys. Res. 103, 5707–5717.
Ravishankara, A.R., 2009. Are chlorine atoms significant tropospheric free radicals? Proc. Natl. Acad. Sci. U. S. A. 106, 13639–13640.
Singh, H.B., Thakur, A.N., Chen, Y.E., Kanakidou, M., 1996. Tetrachloroethylene as an indicator of low Cl atom in the troposphere. Geophys. Res. Lett. 23, 1529–1532.
Spicer, C.W., Chapman, E.G., Finlayson-Pitts, B.J., Plastridge, R.A., Hubbe, J.M., Fast, J.D., Berkowitz, C.M., 1998. Unexpectedly high concentrations of molecular chlorine in coastal air. Nature 394, 353–356.
Stevens, D.J., Spicer, L.D., 1977. Kinetics and mechanism of recoil chlorine atom reactions with ethylene. J. Phys. Chem. 81, 1217–1222.
Thornton, J.A., Kercher, J.P., Riedel, T.P., Wagner, N.L., Cozic, J., Holloway, J.S., Dube, W.P., Wolfe, G.M., Quinn, P.K., Middlebrook, A.M., Alexander, B., Brown, S.S., 2010. A large atomic chlorine source inferred from mid-continental reactive nitrogen chemistry. Nature 464, 271–274.
Wigner, E., 1937. Calculation of the rate of elementary association reactions. J. Chem. Phys. 5, 720–725.
Wingenter, O.W., Blake, D.R., Blake, N.J., Sive, B.C., Rowland, F.S., Atlas, E., Flocke, F.J., 1999. Tropospheric hydroxyl and atomic chlorine concentrations, and mixing timescales determined from hydrocarbon and halocarbon measurements made over the southern ocean. J. Geophys. Res. 104, 21819–21828.
Wright, M.R., 1999. Fundamental Chemical Kinetics and Exploratory Introduction to the Concepts. Ellis Horwood, Chichester, U.K.